

MEMS switches for 0.1–40 GHz for Pico-satellite application

Neelima Kolhare

Received: 25 June 2014 / Accepted: 6 January 2015 / Published online: 6 February 2015
© Springer-Verlag Berlin Heidelberg 2015

Abstract This paper deals with the RF (Radio Frequency)-MEMS (Micro-Electro-Mechanical-System) switches are integrated in CPW topology. Phase shifter is integrated on high resistivity silicon substrate and loading elements are 360 switch design using the coventorware software and its superiority over the existing technologies like PIN Diodes and Field-Effect-Transistors regarding size, power, Isolation The measured down state insertion loss of -0.1 dB up to 40 GHz and switch resistance is 1Ω . The measured reflection coefficient is dominated by t-line switch is -20 dB at 30 GHz. This switch used in X-band and K-band phase shifter, switched capacitor bank and tunable filter. The 1-kg class satellite plans to use the MEMS TxRx switch as a functional component on its RF communication board. Application of switch based Phase shifters for satellite based radars (20 billion cycles), missile systems (0.1–1 billion cycles), long-range radars (20–200 billion cycles). By cutting the mass of components onboard the space vehicle, the launch costs and hopefully the overall budget for production can be reduced.

1 Introduction

Currently, PIN diode or Field Effect Transistor (FET)-based switches are utilized for their high switching speeds, high power handling, low drive voltage, low cost, and technology maturity. MEMS RF technologies offer the advantages of low power consumption (near zero), low insertion loss (~ 0.1 dB up to 40 GHz), and high isolation (>40 dB),

as well as low volume and low mass. In the case of the transceiver, lower insertion loss in the switches between the antenna and the first low-noise amplifier (LNA) leads to lower noise figures and higher sensitivity of the receiver. This effect is magnified when more than one antenna is used, which requires additional switches in the antenna-LNA path. Half duplex systems utilize RF switches to switch between transmit and receive modes. Redundant systems use RF switches to change between redundant segments. Multiple antenna systems, such as diversity receivers or ping-pong mode radar systems, use RF switches for antenna switching.

Virtually all spacecraft with communications or radiometric systems employ such configurations and their performance currently suffers from high insertion loss/low isolation in solid-state RF switches. RF MEMS used in Satellite Communication Systems (12–35 GHz): Switching networks with 4×4 and 8×8 configurations and reconfigurable-Butler matrices for antenna applications (0.1 million cycles), switched filter banks (0.1–100 million cycles, depending on the application). Also, phase shifters for multi-beam satellite communication systems (1–20 billion cycles).

The primary cause of failure in contact MEMS switches is degradation of the contact area metal due to repeated impact between the base and the suspended beam. Pitting, wear, metal migration, and contamination can all contribute to a significant increase in contact resistance and insertion loss. The failure rate is amplified when operating at RF powers over 100 mW because micro welding can bond the pads together, resulting in a permanent short failure

Two key advantages arise when considering MEMS devices in space applications. The first advantage is realized by lowering launch cost. Currently, launching a spacecraft into low Earth orbit (LEO) costs about \$10,000 per

N. Kolhare (✉)
Department of E&TC, Government College of Engineering,
Aurangabad, Maharashtra, India
e-mail: nilima_13@yahoo.com; nilimageca@gmail.com

Table 1 Comparison between various RF Switches

Switch type	Isolation	Insertion loss	Power consumption Power dissipation	Switching time	Linearity
PIN diodes	Medium	Good	More	Good	Poor
FET's	Low	Good	Medium	Excellent	Poor
RF MEMS	0.1 dB	Excellent	500 mW 10–100 nJ	2–100 μ s	Excellent

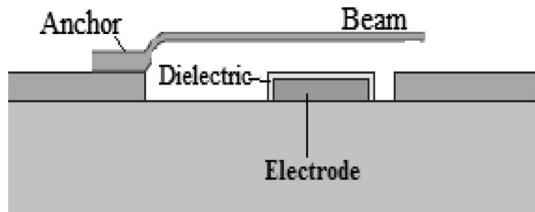


Fig. 1 Series contact switch

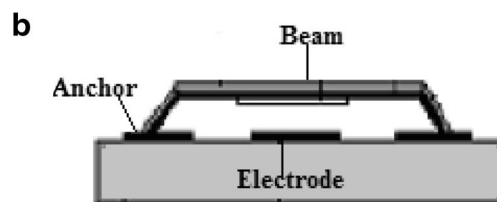
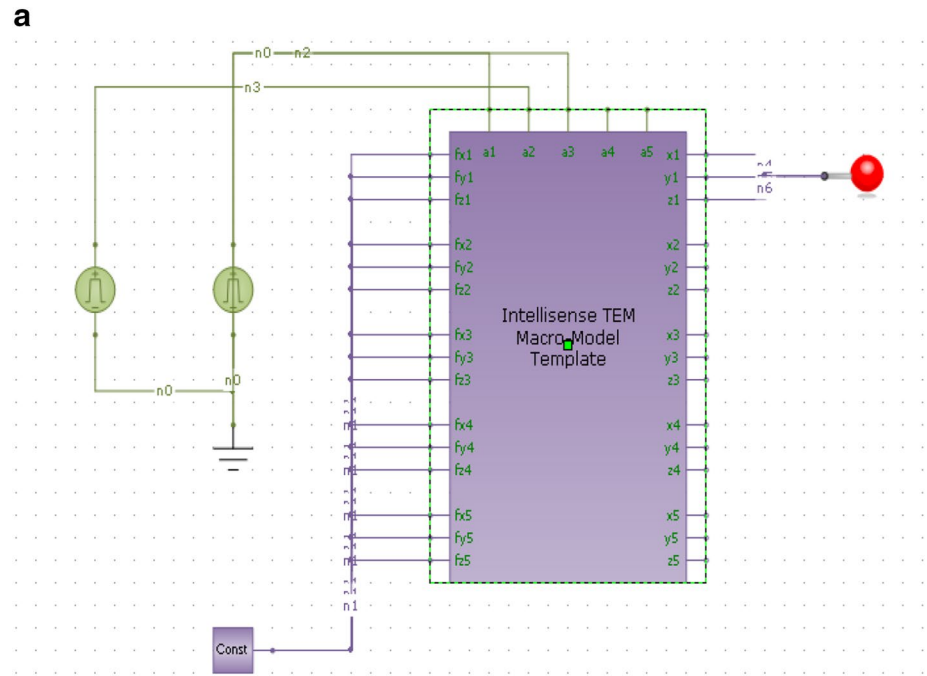
kilogram, and placing a craft into a higher geosynchronous Earth orbit (GEO) costs about \$50,000 per kilogram (Sharma et al. 2013). Obviously, by reducing mass, designers stand to gain in reducing total project cost. The second

advantage is the devices resistance to radiation and vibration. Two key advantages arise when considering MEMS devices in space applications. The first advantage is realized by lowering launch cost. Currently, launching a spacecraft into low Earth orbit (LEO) costs about \$10,000 per kilogram, and placing a craft into a higher geosynchronous Earth orbit (GEO) costs about \$50,000 per kilogram (Sharma et al. 2013).

Obviously, by reducing mass, designers stand to gain in reducing total project cost. The second advantage is the devices resistance to radiation and vibration.

RF MEMS Switches are used for make and break contact between the transmission lines, and operates in the frequency range 0.1 GHz–40 GHz. In the last two decades

Fig. 2 a Shunt capacitive switches. b Shunt capacitive switch



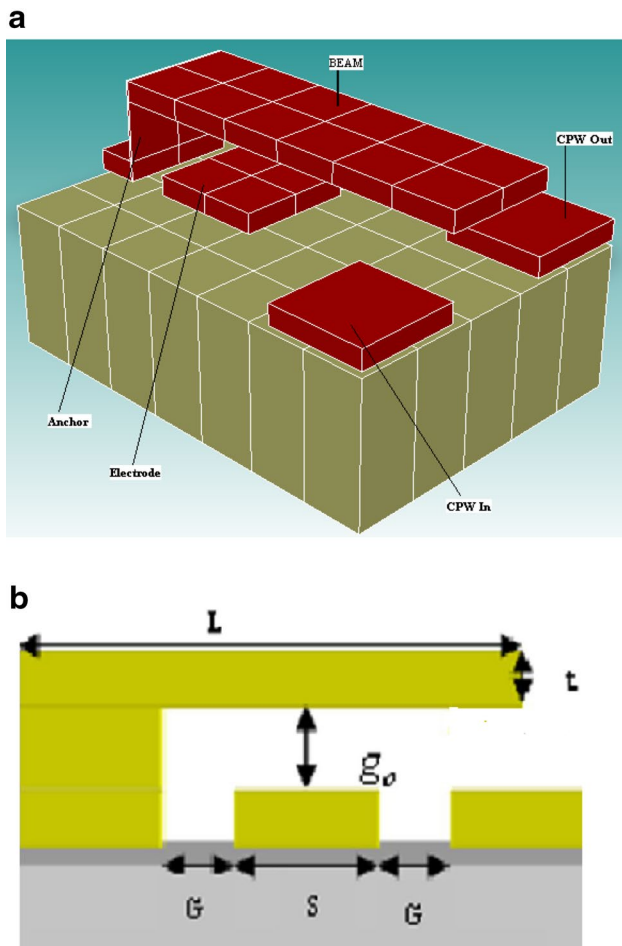


Fig. 3 a Solid cantilever switch. b Side view of cantilever switch

MEMS provided very strong and effective solution in the various passive circuits applications like varactors, switches and in various complex networks like filters.

As per recent generation requirements in terms device should be small in size, should be effective in performance such as low loss, less DC power consumption, less insertion loss and high isolation between the plates and for high frequency applications device should have high Q-factor. These all requirements full filled by the MEMS technology and practically implemented as effective technology for Military applications, mobile, wireless and satellite communications.

The RF MEMS technology dominates over the existing technologies based devices like PIN diodes and FET. As per following characteristics mentioned in the Table 1.

MEMS Switches combine advantages of Mechanical and Semiconductor Switches together and yields the advanced switches which will fulfill all the requirements like small in size, low DC power consumption, lower insertion loss, high off-state isolation (Grant and Mansour 2002).

Because of electromechanical isolation, RF circuit doesn't leak or couple significantly to the actuation circuit.

And electromechanical coupling is done through electrostatically through air less power required because power consumes only when actuation occurs.

Based on MEMS actuation, MEMS switches can be classified by following three characteristics;

- (i) RF circuit configuration
- (ii) Mechanical structure
- (iii) Form of contact.

Basically from a switch contact perspective, there are two types of switches based on the MEMS technology Application point of view- Series Contact Switches and Shunt Capacitive Switches.

1.1 MEMS switches

The cantilever is fabricated using low stress nitride or oxide layer with metal portion at its tips. The metal layer is composed of Au layer and is isolated from another layer by oxide or nitride (Fig. 1).

2 Design parameter

2.1 Model construction: design parameter

2.1.1 Shunt capacitive switches

RF MEMS capacitive shunt switches, a grounded beam is suspended over a dielectric pad on the transmission line. When the beam is in the up position, the capacitance of the line-dielectric-air-beam configuration is on the order of ~50 pF, which translates to a high impedance path to ground through the beam. However, when a dc voltage is applied between the transmission line and the electrode, the induced electrostatic force pulls the beam down to be coplanar with the dielectric pad, lowering the capacitance to pF levels, reducing the impedance of the path through the beam for high frequency (RF) signal and shorting the RF to ground.

The insertion loss of the capacitive switch is lower than 1.2 dB up to 40 GHz, the extracted up-state capacitance is 30 PF and isolation is 1.3, 26, and 27 dB at 1, 20, and 40 GHz respectively. As one end is free it requires lower actuation voltage compared to Air bridge MEMS switch (Brown 1998). The capacitive MEMS switch is as shown in Fig. 2a, b.

2.1.2 RF performance

For designing cantilever beam as an actuator we should know the pull-in voltage, hold down voltage, spring constant for cantilever and the resonant frequency for cantilever. Also

Z- Displacement Results and graph:

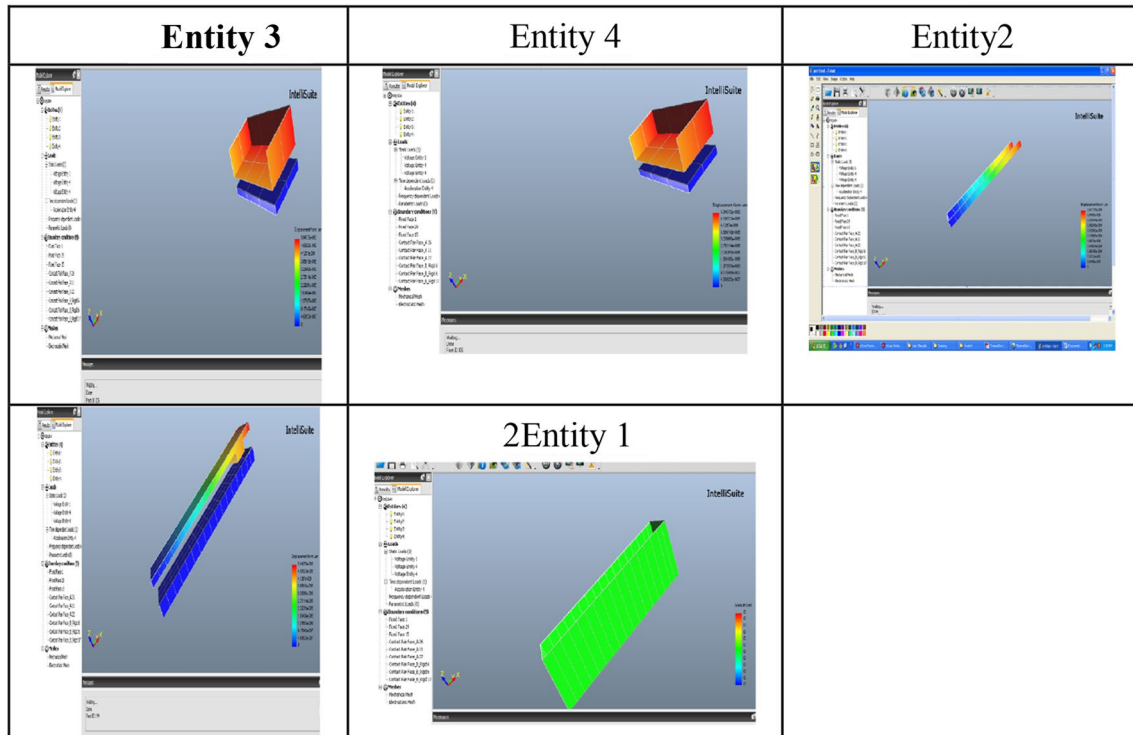


Fig. 4 Displacement/stress (direct integration): displacement result (viewed for different entities separately)

switching lifetime and switching time need to consider. The Solid structure of RF MEMS Cantilever Switch looks as shown in Fig. 3a and its side view is shown in the Fig. 3b.

2.2 Theoretical considerations

2.2.1 Actuation voltage

The working of the cantilever switch is mainly depending on the applied electric field to the electrode V , because of this applied field the electrostatic force F is exerted on the beam, this electrostatic force is measured as in Eq. (1),

$$F = \frac{\epsilon_0 AV^2}{2g^2}, F_r \propto K_t \Delta x \quad (1)$$

where, V is the applied voltage, A is the contact area between electrode and beam and g is the deflected gap between electrode and the beam, and K_t is the spring constant. When the applied voltage goes on increasing the electrostatic force exerted on the cantilever beam is goes on increasing which will tends to beam pull down towards the electrode tends to decreases the gap present between the beam and the electrode.

1. When this applied voltage goes on increases the time comes at certain value of applied voltage beyond that

voltage the electrostatic force F is greater in magnitude than the restoring force which is exerted by the anchor because of the spring constant of that material. At this applied voltage the electrostatic force dominates over the restoring force as shown in the Fig. 4, which pulls down the beam towards the electrode, which will short circuits the input and output line causes the signal to move from input to output. This makes the switch on. In this work we designed the Cantilever switch of length $150 \mu\text{m}$, width of beam (W) $40 \mu\text{m}$, g_0 is $2.2 \mu\text{m}$ and thickness of the beam is $0.7 \mu\text{m}$ from the theoretical pull in voltage is 38.8 V while from Coventorware analysis it is 40 V as shown in the Fig. 5. This voltage at which the beam pulled down towards the electrode is called as the pull-in voltage V_p and is given by (Hung and Senturia 1999) (Senturia and Osterberg 1997) the Eq. (2) as,

$$V_p = \sqrt{\frac{8K_t g_0^3}{27 \epsilon_0 A}} \quad (2)$$

where K_t is the spring constant of the beam material, g_0 is the original gap between the beam and the electrode and ϵ_0 is the permittivity of the material. The spring constant K_t is calculated by the Eq. (3) as,

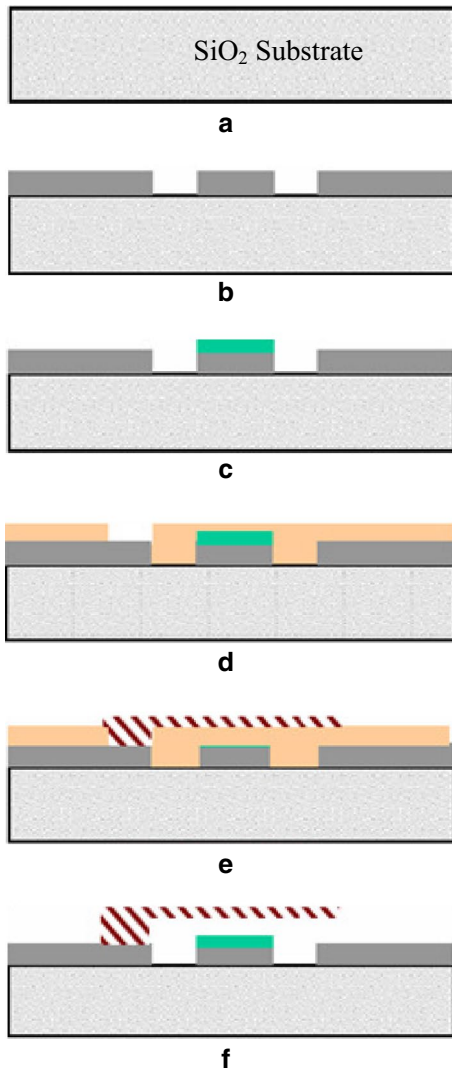


Fig. 5 Explains fabrication process of cantilever type switch. **a** Substrate, **b** Actuated electrode formation, **c** Deposition of SiN₃, **d** Deposition of sacrificial layer, **e** Deposition of metal, **f** Deleting sacrificial layer

$$K_t = \frac{EWt^3}{4l_m^3} \tag{3}$$

where, E is the young’s modulus of the material, t is the thickness of the beam and l_m is the enforced length of the beam is given by the Eq. (4) as,

$$l_m = l - W - l_s \tag{4}$$

where l the length of the beam, W is the width and l_s is the isolation length of the beam. The movement of the cantilever beam switch because of the applied voltage is as shown in the Fig. 6 (Graph 1). Initially as the applied voltage goes on increases the gap between the beam and ground electrode gradually reduces, after the gap becomes 2/3 of original gap cause the beam suddenly pull downs,

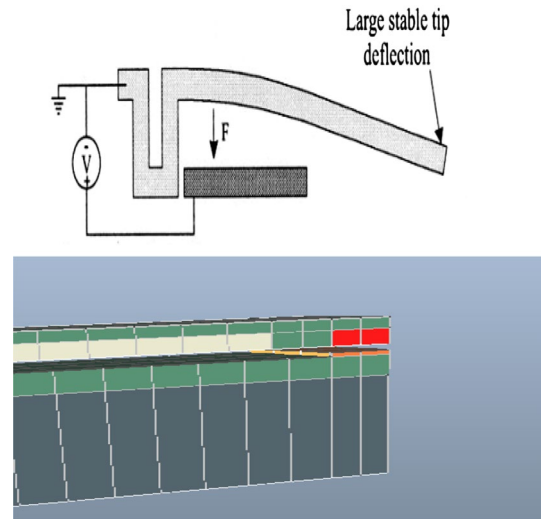
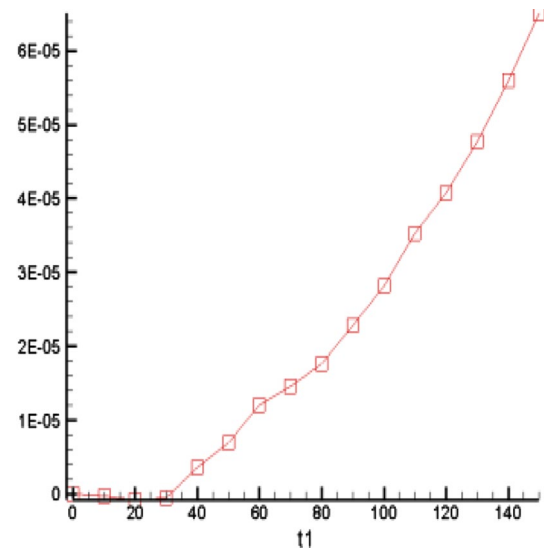
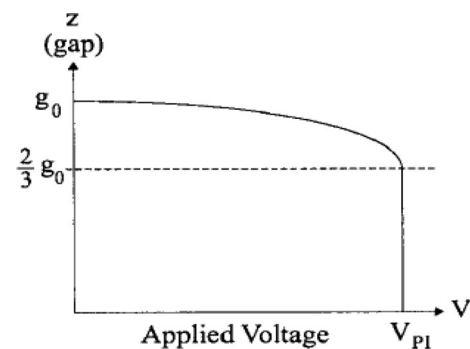


Fig. 6 Movement of cantilever switch verses applied voltage

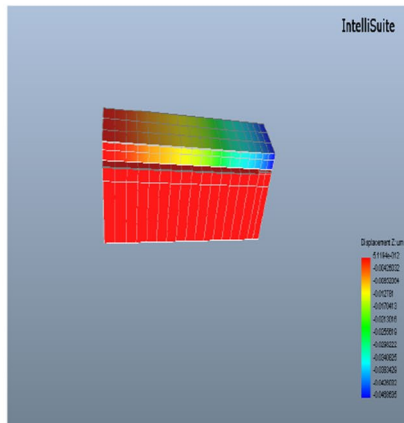


Graph 1 Graph between actuator deflection and applied voltage



Graph 2 Graph of voltage vs displacement of beam

2. Displacement:



Pull in voltage: = 38 V

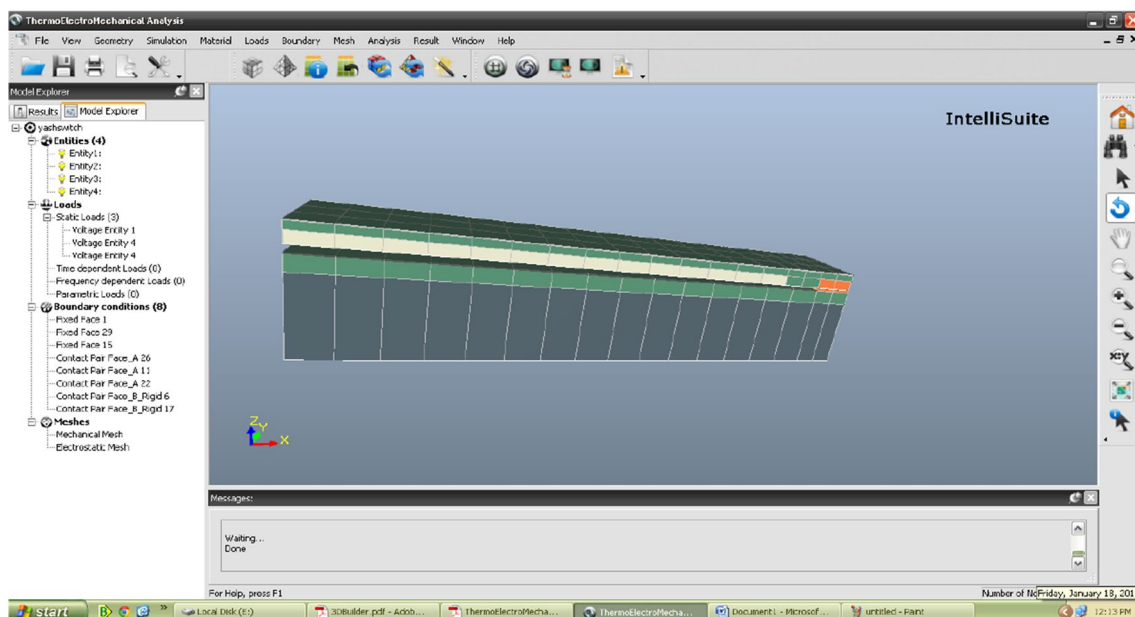
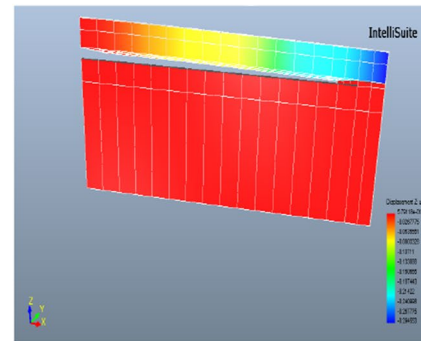


Fig. 7 Displacement of tip of beam

is shown in Graph 2 and the Fig. 7 represents the voltage required to pull down the cantilever beam to make switch as an on. The Graph 3 shows the electrostatic force exerted by the applied voltage to the electrode.

Also from the different analysis on the structure it is observed that the actuation voltage required pulling the beam downward to make switch on is varies according to the length of the beam and also by Varying area of the actuated electrode. This is shown in the Table 2.

2.3 Switching times

Using 4-point resistance measurement and the laser vibrometer the electrical resistance and mechanical displacement

of the switch is measured as a function of time. The closing time depends on the actuation voltage and the opening time depends on the mechanical properties of the switch. By scaling the MEMS devices the switching time is also scale downs, as $t_s = 10.6$ and $4 \mu\text{s}$ (Au and Al beams)

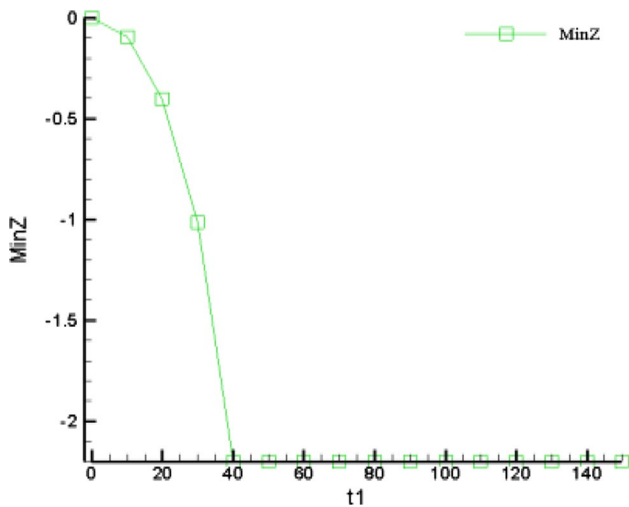
$$t_s \approx 3.67 \frac{V_p}{V_s \omega_0}, f_0 = \sqrt{\frac{K}{m}} \quad (5)$$

where (ω_0, f_0) is resonant frequency, V_p is pull-in voltage and V_s is applied voltage.

2.4 Up state capacitance

S parameter is measured in up state position

$$C_{pp} = \varepsilon w W / (g + t_d / \varepsilon_r)$$



Graph 3 Applied Voltage versus electrostatic force on the beam

Table 2 Specification of RF switch

Length of MEMS beam	$l = 300 \mu\text{m}$,
Thickness	$t = 0\text{--}2 \mu\text{m}$
Pull down electrode length width	$W = 100 \mu\text{m}$
Bridge width	$w = 100 \mu\text{m}$
Gap height	$0.5\text{--}3 \mu\text{m}$
Spring constant	$k = 10 \text{ N/m}$
Residual stress	(Au and Al) 9.5 MPa
Mechanical resonant frequency	$f_0 = 103 \text{ kHz}$
Switch time	$4/10 \mu\text{s}$
Capacitive ratio	$80\text{--}120$
Intermodulation	66 dBm , Loss = -0.07 ($10\text{--}40 \text{ GHz}$)
Isolation [dB]	-20 (10 GHz), -35 (30 GHz)
Modulus of elasticity, $E \pm 3 \text{ GPa}$	190
Density, $190 \rho \pm 0.05 \text{ g/cm}^3$	2.33

$$\Phi \text{ phase delay} = j\omega C_u Z_0 / 2 = 0.897 \text{ rad}$$

$$S_{11} = (-j\omega C_u Z_0) / (2 + j\omega C_u Z_0)$$

2.5 Down capacitance

S_{21} is measured when capacitance is in the down positions

$$S_{21} = 1 - (j\omega C_u Z_0) / 2 = 1.32$$

$$C_d = \epsilon_0 \epsilon_r w W / (g + t_d / \epsilon_r)$$

3 Device fabrication process

In the fabrication process of the cantilever switch is explained roughly step by step as bellow,

3.1 Substrate creation

To form the cantilever type structure we require the platform is called the substrate, silicon dioxide (SiO_2) material used as the substrate. In this design the substrate of $150 \mu\text{m}$ length, $110 \mu\text{m}$ width and $5 \mu\text{m}$ thickness is used.

3.2 Electrode formation

With the help of generic plasma enhanced chemical vapor deposition (PECVD) and generic dry etching process, electrode is formed by exposing the part of the deposited electrode material through the openings in the masking layers and removes the unnecessary material. In this design Aluminum material is used for the electrode purpose, as shown in Fig. 5b.

3.3 Deposition of silicon nitride layer

To avoid the stiction problem, arises in the metal to metal contact occurs which affects on the smooth switching operation without this layer. In this design $0.2 \mu\text{m}$ thick SiN_3 layer is deposited over the electrode by PECVD process, as shown in Fig. 5c.

3.4 Sacrificial layer formation

To make the cantilever beam over the free space and separation between the CPW lines, BPSG material is used of $2.2 \mu\text{m}$ in height as shown in the Fig. 5d.

3.5 Forming cantilever beam

By using low chemical vapor deposition (LPCVD) $0.7 \mu\text{m}$ thickness and $2.2 \mu\text{m}$ height Aluminum cantilever beam is formed, as shown in the Fig. 5e.

3.6 Removing the sacrificial layer

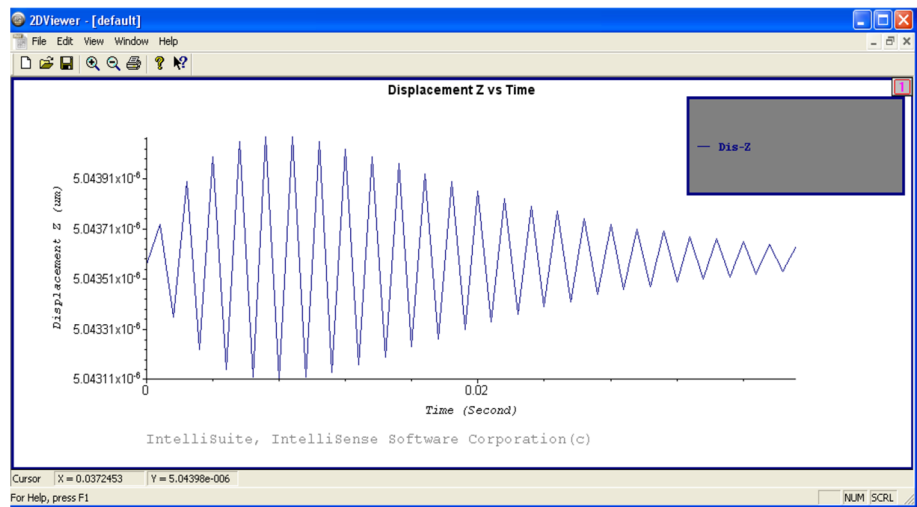
After cantilever beam structure formation the BPSG material is deleted to make the beam free in the air by using plasma etching process, as shown in Fig. 5f.

4 Results and discussion

4.1 Analysis and their results

We have simulated and analysis different structure of RF Switches with cantilever, we conclude that cantilever configuration and dimension determine the membrane performance when its material has been decided (Graph 4).

Fig. 8 Switch bouncing



Displacement:

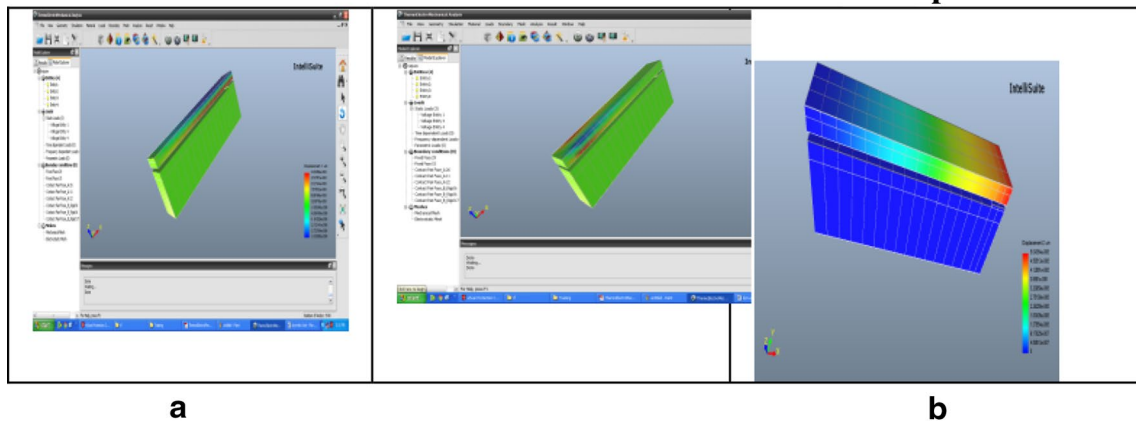
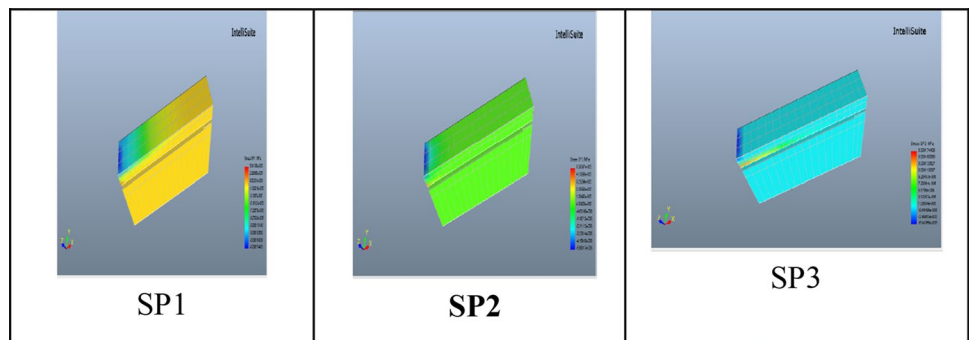


Fig. 9 **a** Displacement for frequency analysis X, Y and Z Displacement (Y displacement is not significant. It takes place due to elastic nature of aluminum). **b** Graph of Z displacement vs time

Fig. 10 Observed reaction forces for different axes is observed. Reaction forces in the Z direction is more significant than X and Y directions



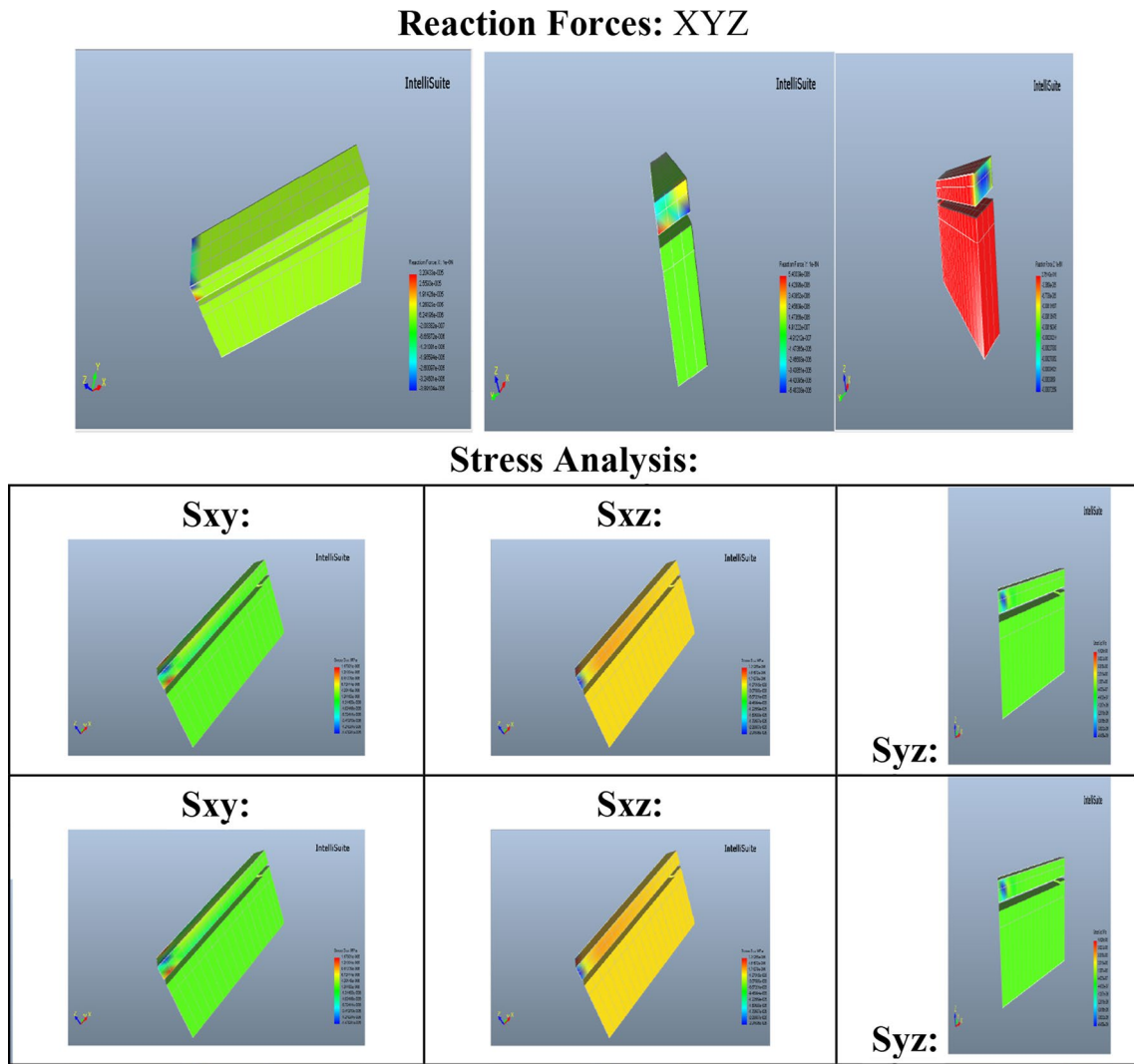


Fig. 11 Stress/Displacement/Electrostatic (direct integration): here distribution of stress in different Planes is observed. Szz (forces in z-z plane) is greatest

4.2 Static analysis: thermo electromechanical relaxation deformed shape

4.2.1 Dynamic analysis

Effect of pressure The pressure of the environment in which the sensor can affect the results produced. If the pressure of the environment increases, the dynamic viscosity of the damping fluid increases. This increase in damping reduces the Q-value and can also reduce the deflection of the cantilever which both, in turn, decreases the data quality and reliability. In addition to changing the damping, an increase in pressure will also alter the concentration of the gas in the environment, which can affect the absorption rate, and equilibrium giving shifted results (Figs. 8, 9).

Feature of extract planar data Distribution of stress is observed for 3 different modes: b. Stress invariant analysis: [Analysis type: displacement/stress (mode based)] (Figs. 10, 11)

4.3 Frequency analysis

4.3.1 Static stress

Natural freq result Natural frequency is the fundamental frequency of the switch. For us, mode 1 is most significant. Here the natural frequency is 118 kHz. That means, the switching time for the designed switch is 8.33 μs. Theoretical value is around 10 μs.

capacitance is important for us. It is 5.13 nF

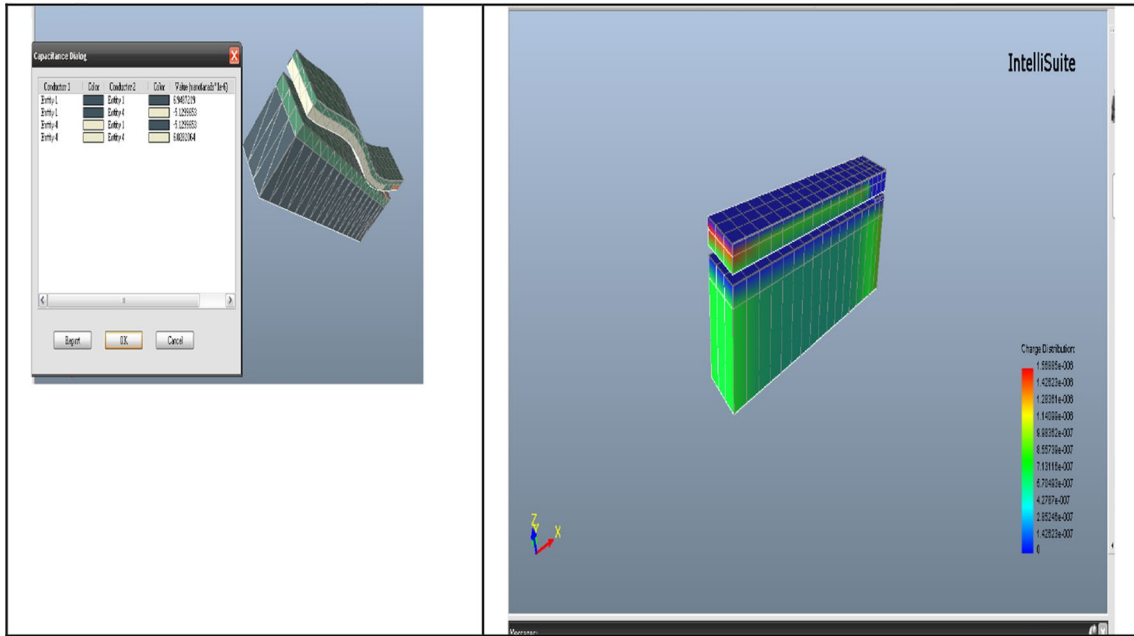


Fig. 12 Charges density and C–V characteristics

Fig. 13 Pressure distribution

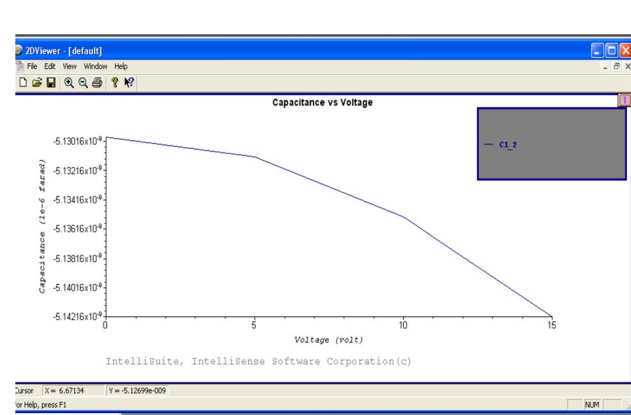
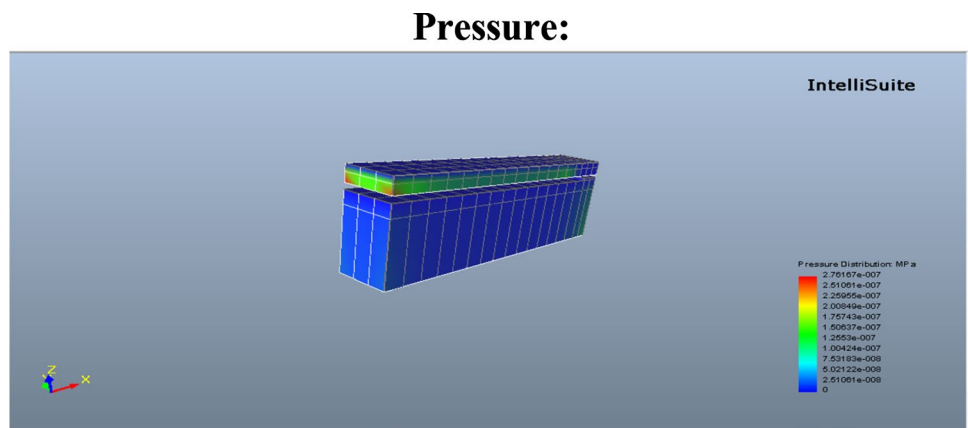
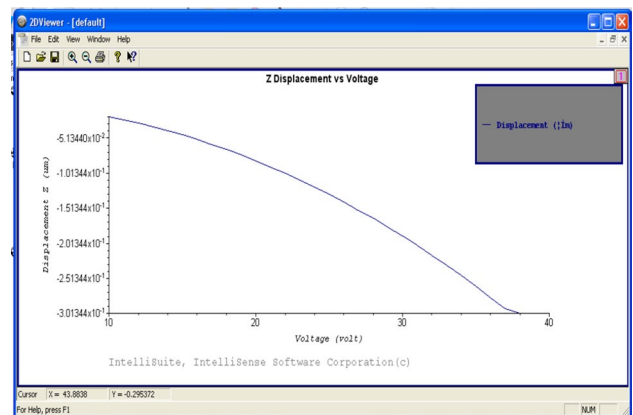
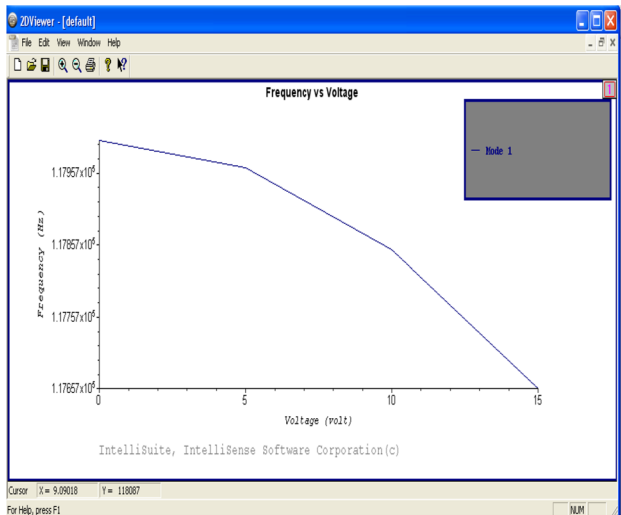


Fig. 14 Capacitance vs Voltage



Graph 4 Electrostatic force vs Displacement



Graph 5 Frequency vs Voltages

Table 3 Shows different lengths beam and the required pull in voltage

Length of beam (μm)	Pull in voltage V_p (v)
150	40
180	16
200	11
250	7
280	5

Table 4 CV characteristics and model analysis, transient analysis

Charge (x10e-06)	Capacitance	Modes	Natural frequency (KHz)
1.508	2.76167E-07	Mode 1	117.385
1.428	2.5116E-07	Mode 2	740.637
1.280	2.259E-07	Mode 3	1,432.95 K
1.145	2.008E-07	Mode 4	1,802.3 K
0.9.985	1.757E-07	Mode 5	2,083.92 K
0.8567	1.506E-07		
0.7131	1.004E-07		
0.57047	0.759E-07		
0.42787	0.5029E-07		
0.28512	0.251E-07		
0	0		

4.3.2 Capacitance

Capacitor is created between two conductors due to the potential difference [entity 4 (15 V) and entity 1 (0 V)].

This table shows the self capacitance and mutual capacitance between entity 4 and entity 1. Mutual capacitance is important for us. It is 5.13 nF (Figs. 12, 13)

Charge distribution is seen in the entities where the potential is applied (Fig. 14).

Pressure distribution is observed in the part where reaction forces are more (Graphs 4, 5).

4.3.3 Thermoelectromechanical relaxation

As actuation voltage goes on increasing, the natural frequency decreases Tables 3, 4.

5 Conclusion

In this Paper presented electromagnetic model of MEMS switch. Pull down voltage 5 V is achieved with design for a gap height of 1–4 μm . The low spring constant has shown excellent characteristic up to 40 GHz with a low insertion loss (–0.1 dB up to 30 GHz). Isolation of –40 dB is achieved at 0.1–5 GHz and decreases –20 dB at 40 GHz. Static and dynamic analysis has described in this paper.

Acknowledgments The devices were simulated in the NPMAS Laboratory at the Physics department of Dr. Babasaheb Ambedkar Marathwada University, Aurangabad as NMDC National mems design center. The authors would like to thank SSPL, DRDO, at Nanotechnology for scheduling film depositions, for calibrating RF Switches used in device testing and for advice given for vacuum pressure sensing, and I would like to thanks NPMAS for providing Intellisuit software and necessary guidance Prof. A. G. Murugkar for their proper suggestions. Also to our vice chancellor Dr. V. M. Pandharipande sir for allowing me to use MEMS laboratory for my work.

References

Brown ER (1998) RF MEMS switches for reconfigurable integrated circuits. *IEEE Trans Microwave Theory and Techniques* 46(11): 1868–1880

Charalampidis N, Kampitaki D (2009) “On the design of an ohmic RF MEMS switch for reconfigurable microstrip antenna applications”

Grant PD, Mansour RR (2002) A comparison between RF MEMS switches and semiconductor switches. *Can J Elect Comput Eng* 27(1):33–39

Hung ES, Senturia SD (1999) Extending the travel range of analog-tuned electrostatic actuators. *J Microelectromech Syst* 8: 847–805

Senturia SD, Osterberg PM (1997) M-TEST: a test chip for MEMS material property measurement using electrostatically actuated test structures. *J Microelectromech Syst* 6(2):107–118

Sharma AK, Balaji CG, Singh SG (2013) Ohmic RF MEMS switch with low loss and low force on quartz for reconfigurable circuits 3(1): 45–54